Melting, Crystallization Behaviors, and Nonisothermal Crystallization Kinetics of PET/PTT/PBT Ternary Blends

Mingtao Run,[1] Aijun Song,[2] Yingjin Wang,[1] Chenguang Yao[1]

[1]*College of Chemistry and Environmental Science, Hebei University, Baoding 071002, China*
[2]*Department of Chemistry, Hebei Normal University of Science and Technology, Qinhuangdao 06660, China*

Received 6 March 2006; accepted 2 January 2007
DOI 10.1002/app.26147
Published online 8 March 2007 in Wiley InterScience (www.interscience.wiley.com).

ABSTRACT: The melting, crystallization behaviors, and nonisothermal crystallization kinetics of the ternary blends composed of poly(ethylene terephthalate), poly(trimethylene terephthalate) (PTT) and poly(buthylene terephthalate) (PBT) were studied with differential scanning calorimeter (DSC). PBT content in all ternary blends was settled invariably to be one-third, which improved the melt-crystallization temperature of the ternary blends. All of the blend compositions in amorphous state were miscible as evidenced by a single, composition-dependent glass transition temperature (T_g) observed in DSC curves. DSC melting thermograms of different blends showed different multiple melting and crystallization peaks because of their various polymer contents. During melt-crystallization process, three components in blends crystallized simultaneously to form mixed crystals or separated crystals depending upon their content ratio. The Avrami equation modified by Jeziorny and the Ozawa theory were employed to describe the nonisothermal crystallization process of two selected ternary blends. The results spoke that the Avrami equation was successful in describing the nonisothermal crystallization process of the ternary blends. The values of the $t_{1/2}$ and the parameters Z_c showed that the crystallization rate of the ternary blends with more poly(ethylene terephthalate) content was faster than that with the lesser one at a given cooling rate. The crystal morphology of the five ternary blends investigated by polarized optical microscopy (POM) showed different size and distortional Maltese crosses or light spots when the PTT or poly(ethylene terephthalate) component varied, suggesting that the more the PTT content, the larger crystallites formed in ternary blends. © 2007 Wiley Periodicals, Inc. J Appl Polym Sci 104: 3459–3468, 2007

Key words: poly(ethylene terephthalate); poly(trimethylene terephthalate); poly(buthylene terephthalate); DSC; crystallization

INTRODUCTION

Poly(trimethylene terephthalate) (PTT) commercialized until 1990s by Shell Chemicals, an important new member of the polyester family, is relatively new linear aromatic polyester with three methylene units in its chemical structure.[1] Many properties of PTT are between those of poly (ethylene terephthalate) (PET) and poly (buthylene terephthalate) (PBT), e.g., its mechanical properties are comparable with that of PET whereas its processing characteristics are similar to that of PBT. Thus it combines the two key advantages of PET and PBT into one polymer. It has an important application in the textile industry[2] and has been a promising engineering thermoplastic.[3]

Recently, there has been much research on the crystallization and rheological properties of PTT and blends of PTT with other polymer materials.[4–15] Chuah[7] and Hong et al.[8] investigated the isothermal crystallization behavior of PTT using the Avrami equation and suggested that the crystallization rate of PTT was between that of PET and PBT when they were compared at same degree of under cooling rate. Xue et al.[9] studied the nonisothermal crystallization behavior of PTT using Avrami equation modified by Jeziorny, Ozawa equation and the combined equation of Ozawa and Avrami, and found out that these methods were available for the analysis of the crystallization behavior of PTT.

Because of the similarity in chemical structure of PET, PTT, and PBT, studies on crystallization and rheological behaviors of binary blends of these three linear aromatic polymers have been receiving much attention. Kang[10] investigated the rheological and thermal properties of the blends of PET/PBT. Jacques[11] and Song and White[12] studied various aspects for blends of PET/PBT. Yang[13] and Ou et al.[14] studied various aspects for blends of PET/PTT. Supaphol et al.[15] investigated the nonisothermal melt-crystallization kinetics for PTT/PBT blends applying Avrami, Ozawa, and Ziabick models and indicated that both the Avrami and Ozawa macrokinetic models provided a satisfactory description of the experimental data.

Investigations of the kinetics of polymer crystallization in product processing are of great importance in both theoretically and practically. Therefore,

Correspondence to: M. Run (rmthyp@hotmail.com).
Contract grant sponsor: Science Foundation of Hebei University; contract grant number: Y2006065.

understanding the interrelationships of the materials among of processing-structure-property exactly became very meaningful. However, so far, to the best of our knowledge, there are few reports on the melting and crystallization behavior of PET/PTT/PBT ternary blends. In this study, various ternary blends of PET/PTT/PBT were prepared, in which the content of PBT in blends was settled invariably to be one-third to improve the crystallization and rheological properties of the ternary blends. Their melting, melt-crystallization behaviors, especially the nonisothermal crystallization kinetics were investigated using differential scanning calorimeter (DSC). The Avrami equation modified by Jeziorny and Ozawa model were employed to describe the nonisothermal crystallization process of the PET/PTT/PBT blends. The crystal morphology of different blends was also studied by the polarized microscopy.

THEORETICAL BACKGROUND

The relative crystallinity ($X_c(t)$) as a function of time is defined in the following equation:

$$X_c(t) = \frac{\int_{t_0}^{t} (dH_c/dt)dt}{\int_{t_0}^{t_\infty} (dH_c/dt)dt} = \frac{A_0}{A_\infty} \quad (1)$$

where t_0 and t_∞ are the time, at which crystallization starts and ends, and A_0 and A_∞ are areas under the normalized DSC curves. The half-time of crystallization ($t_{1/2}$) is the time required for the completion of 50% crystallization completed. Generally, the smaller the value of $t_{1/2}$, the faster the crystallization rate is.

The Avrami theory modified by Jeziorny

The Avrami theory[16] has been widely used for the interpretation of the isothermal crystallization process:

$$1 - X_c(t) = \exp(-Z_t t^n) \quad (2)$$

$$\log[-\ln(1 - X_c(t))] = n \log t + \log Z_t \quad (3)$$

where $X_c(t)$ is the relative degree of crystallinity at time t; the exponent n is a mechanism constant with a value depending on the type of nucleation and the growth dimension, and the parameter Z_t is a growth rate constant involving both nucleation and growth rate parameters. The exponent n and Z_t can be obtained from the slope and intercept of the line in the plot.

Although, the physical meanings of Z_t and n cannot be related to the nonisothermal case in a simple way, it can also been used to describe nonisothermal processes,[17] and their use provides further insight into the kinetics of nonisothermal crystallization. The crystallization time t can be obtained by the following equation:

$$t_c = \frac{T_s - T}{|D|} \quad (4)$$

where T is the temperature of crystallization time t_c, T_s is the temperature at which crystallization starts, and D is the cooling rate. From the Eqs.(3) and (4), we obtain:

$$\log[-\ln(1 - X_c(t))] = n \log\left(\frac{T_s - T}{|D|}\right) + \log Z_t \quad (5)$$

Considering the nonisothermal characteristics of the process investigated, the parameters for the value of the crystallization rate, Z_t, should be corrected by the cooling rate D, because the temperature is constantly changing during the process. The parameter characterizing the kinetics of nonisothermal crystallization is given by Jeziorny as follows:

$$\log Z_c = \frac{\log Z_t}{|D|} \quad (6)$$

where Z_c is the kinetic crystallization rate constant.

The Ozawa theory

Ozawa extended the Avrami equation to the nonisothermal condition. Assuming that the nonisothermal crystallization process may be composed of infinitesimally small isothermal crystallization steps, the following equation is derived:

$$1 - X_c(T) = \exp\left[-\frac{K(T)}{|D|^m}\right] \quad (7)$$

$$\log[-\ln(1 - X_c(T))] = \log K(T) - m \log |D| \quad (8)$$

where $K(T)$ is a function related to the overall crystallization rate that indicates how fast crystallization proceeds, and m is the Ozawa exponent that depends on the dimension of crystal growth. According to Ozawa's theory[18], the relative crystallinity, $X_c(T)$, can be calculated from these equations. By drawing the plot of $\log[-\ln(1 - X_c(T)]$ versus $\log |D|$ at a given temperature, we should obtain a series of straight lines if the Ozawa analysis is valid, and the kinetic parameters m and $K(T)$ can be derived from the slope and the intercept, respectively.

EXPERIMENTAL

Materials

The homopolymers of PTT, PET, and PBT used in this study were supplied by Shell Chemicals (USA),

Tianjin Petrochemical (China), and Yizheng Petrochemical (China), respectively. All these samples were in pellet form, and their intrinsic viscosity were measured in phenol/tetrachloroethane solution (50/50, w/w) at 25°C.

Blends preparation

The materials were dried in a vacuum oven at 140°C for 12 h before preparing blends. The dried pellet of PET, PTT, and PBT were mixed together in different weight ratio as follows: (PET/PTT/PBT) B1: 10/50/30; B2: 20/40/30; B3: 30/30/30; B4: 40/20/30; B5: 50/10/30, and then it was melt-blended in a ZSK-25WLE WP self-wiping, corotating twin-screw extruder, operating at a screw speed of 60 rpm and at a die temperature of 280°C. The resultant blend ribbon was cooled in water, cut up, re-dried before being used in DSC and polarized optical microscopy (POM) measurements. To keep the same thermal processing conditions, three pure pellets of PET, PTT, and PBT were also processed in the twin-screw extruder under the same processing conditions as those of the blends.

Differential scanning calorimeter

The melting and subsequent crystallization behaviors of three pure polymers and various ternary blends were studied by the Perkin–Elmer Diamond DSC instrument that was calibrated with indium prior to performing the measurement, and the weights of all samples were ~8 mg. The samples were heated to 280°C at 100°C/min under a nitrogen atmosphere, and was allowed to stand for 5 min, then quenched to −50°C at a cooling rate of 100°C/min, then heated them to 280°C at a heating rate of 10°C/min, and finally the molten was cooled to −50°C at a cooling rate of 10°C/min. The second heating and cooling process were recorded, respectively. It is necessary to illuminate that the above process is consecutive.

The nonisothermal crystallization behaviors of the selected blends B1 and B5 were performed as follows: the sample was heated to 280°C in nitrogen, held for 5 min and then cooled to 50°C at constant cooling rates of 5, 10, 15, 20, 30°C/min, respectively. The exothermic curves of heat flow as a function of temperature were recorded and investigated.

Polarized optical microscopy

The crystal morphology of the five ternary blends were performed by Yongheng 59XA-POL (China) with a hot-stage and a Panasonic digital camera. Samples were prepared by sandwiching a tiny pellet of the blend between two glass plates, compressing on hot-stage at 280°C for 5 min and then cooling to room temperature at a cooling rate of 2°C/min, and then took photographs by camera.

RESULTS AND DISCUSSION

Melting and melt-crystallization behavior

Much of the research work has been focused on the structure-crystallization property relation for three linear aromatic polyesters.[19–23] It is generally believed that the more the number of methylene groups in the repeated union of molecular chains (i.e., 2, 3, and 4 for PET, PTT, and PBT, respectively) are, the lower the melting point is, and the higher is the melt-crystallization temperature. The melting and subsequent crystallization curves of pure PET, PTT, and PBT at the cooling rate of 10°C/min are shown in Figure 1, and the parameters are listed in Table I. From Figure 1, the glass transition temperatures, T_g, are observed obviously for pure PET and PTT at ~78.1 and 43.2°C, whereas that of PBT is inconspicuous at ~39.8°C. The cold crystallization peak temperature T_{cc} for both PET and PTT are observed at ~150.2 and 71.3°C, whereas that of PBT is not observed, which suggests that PBT is able to crystallize fast enough during quenching the sample from a fusion temperature of 280°C to −50°C at 100°C/min. The melting peak temperatures (T_m) for PET, PTT, and PBT are observed at ~249.8, 224.6, and 222.3°C, respectively.

When the melt of the three polyesters are cooled to −50°C at 10°C/min, the plain PBT shows a higher melt-crystallization peak temperature T_{ch} at ~199.2°C than those of PET (T_{ch} = 189.9°C) and PTT (T_{ch} = 172.6°C). The half-time of the crystallization $t_{1/2}$ [the time when the crystallinity is 50%, which

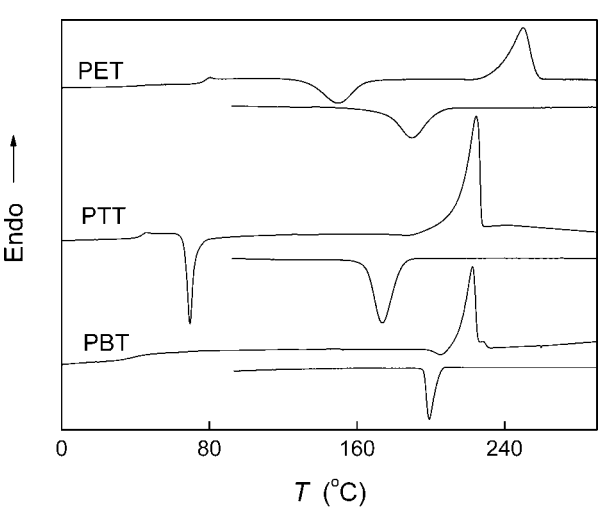

Figure 1 DSC melting and subsequent melt-crystallization thermograms of pure PET, PTT and PBT during heating and cooling rate of 10°C/min.

TABLE I
Physical Properties of the Pure PET, PTT, and PBT Processed on the Twin-Screw Extruder

Sample	Density (g/cm^3)	[η] (dL/g)	M_v	T_g (°C)	T_{cc}[a] (°C)	T_m (°C)	T_{ch}[b] (°C)	$t_{1/2}$ (s)
PET	1.40	0.66	70,000	78.1	150.2	249.8	189.9	161.2
PTT	1.35	0.92	100,400	43.2	71.3	224.6	172.6	108.6
PBT	1.34	1.04	116,600	39.8	—	222.3	199.2	53.5

[a] The temperature of cold crystallization peak in the heating scan.
[b] The temperature of melt-crystallization peak in the cooling scan.

can be derived from the curve of relative crystallinity versus time, e.g., Fig. 5(a,b)] of PET is 161.2 s, followed by PTT (108.6 s) and PBT (53.5 s), indicating that the crystallization rate of PBT is faster than those of PTT and PET. The reason for this is that the four-methylene groups in PBT lead to a quicker arraying of the molecular chains into folded state at a higher temperature in the cooling process than PTT and PET. Generally speaking, the melt-crystallization temperature (T_{ch}) increases with the increase of number of methylene in the chemical structure. But in this study, the T_{ch} of PTT is lower than that of PET though the number of the methylene in PTT is larger. The reason for this is that the physical property of the aromatic polyesters is related to the odd number or even number of methylene groups in the repeated units of molecular chains, which is so-called odd carbon effect. The repulsion between two-closed carbonyl makes them conform in 120° other than 180°,[24] therefore, the PTT molecular chains arrange as the distinctive helical conformation substitute for a plane, and the conformation of PTT is of a special ''Z'' shape.[25] Because of the special chemical structure of PTT molecular, its physical properties change a lot, and its melt-crystallization temperature is lower than that of PET.

Figure 2(a,b) show the melting and subsequent melt-crystallization curves of five ternary blends with various components, and the physical parameters are listed in Table II. From Figure 2(a), only a single and composition-dependent glass transition temperature T_g, which is located between those of the three pure components, is clearly seen in DSC curve of each ternary blend, suggesting a good miscibility between the three polymers in the amorphous state. However, there is no cold-crystallization peak observed in each melting thermogram, suggesting that all of the ternary blends are able to crystallize fast enough during quenching the sample from a fusion temperature of 280°C to −50°C at 100°C/min. This result may be caused mainly by the component of PBT that has a fast crystallization rate.

From Figure 2(a) and Table II, all endotherms exhibit two predominant melting peaks: peak I at higher temperature and peak II at lower temperature relatively, and both of them are variable by composition-dependent. The peak I shift little to higher temperature, while peak II shift little to lower temperature with increasing PET content. Moreover, at this heating rate, the intensity of peak I increases with the increase of PET content, whereas that of peak II decreases with the increase of PET content. Therefore, judging from the melting behavior of the three

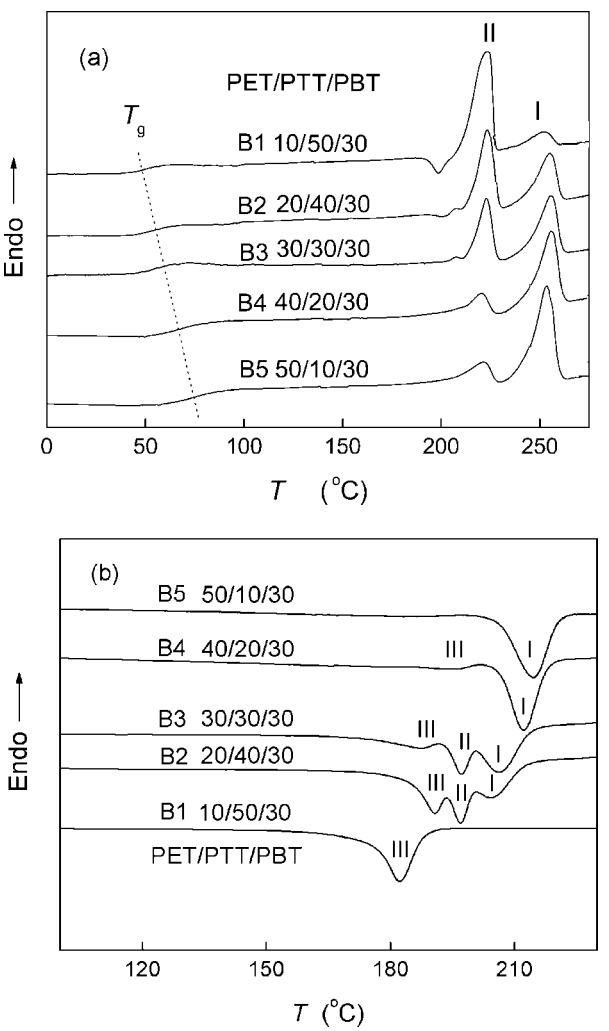

Figure 2 (a) DSC cold crystallization and melting thermograms for quenched PET/PTT/PBT ternary blends recorded during heating at 10°C/min, and (b) DSC melt-crystallization exotherms for PET/PTT/PBT ternary blends recorded during cooling at 10°C/min.

TABLE II
Parameters of PET/PTT/PBT Ternary Blends During the Melting Process and Subsequent Crystallization Process

	Melting process				Crystallization process			
Samples	T_g (°C)	T_{mI} (°C)	T_{mII} (°C)	ΔH_m (J/g)	T_{chI} (°C)	T_{chII} (°C)	T_{chIII} (°C)	ΔH_c (J/g)
B1	50.6	251.2	222.9	41.3	—	—	182.2	−43.0
B2	54.1	255.0	223.8	44.9	204.6	196.9	190.6	−49.0
B3	56.9	255.4	222.9	44.3	206.6	205.7	187.4	−52.1
B4	66.8	255.5	220.6	51.0	212.2	—	195.1	−40.1
B5	73.7	254.8	221.4	53.8	214.8	—	—	−42.0

pure polymers in Figure 1, peak I is the melting behavior of PET, and peak II at lower temperature should correspond to the melting of PTT and PBT or their mixed crystals respectively. It should be noted that the observed T_{mII} of peak II for both PBT and PTT components are in close proximity to each other. The total melting enthalpy of the five ternary blends from B1 to B5 ranges from 41.3 to 53.8 J/g with various PET contents.

From Figure 2(b) and Table II, a single and composition-dependent exotherm is clearly seen in each DSC curve of B1 and B5 samples, with the melt-crystallization temperature T_{chIII} and T_{chI} at ~182.2 and 214.8°C, respectively. Compared with the T_{ch} of the pure PTT (176.5°C) and PET (193.0°C), T_{chIII} of B1 and T_{chI} of B5 are much higher in value. For the PET component in B5 blend, both PTT and PBT components with flexible molecular chains may be plasticizers, which dilute the concentration of PET and improve the arrangement behavior of PET molecular chains; as a result, the crystallization of PET starts at higher temperature. On the other hand, for the PTT component in B1 blend, both PET and PBT crystallized at higher temperature may be heterogeneous nucleus that will improve the crystallization of PTT; as a result, the crystallization of PTT starts at higher temperature. Moreover, PBT component that has a higher melt-crystallization temperature (200.4°C) can also increase the crystallization temperature of both PET and PTT. However, in these two blends of low contents of the minor component, observation of the single crystallization exotherm suggests that even though the minor phase could form its own crystalline phase during melt-crystallization, the amount of the crystalline phase of the minor component, as compared with the amount of the crystalline phase of the major component formed, may not be enough to show its distinctive crystallization exotherm in DSC curves.

In the DSC curves of the B2 and B3 blends, the observation of three crystallization peaks (peak I, peak II, and peak III) confirms that each component of the ternary blends forms their own crystals during cooling scan. According to the data T_{ch} of the pure PET, PTT, and PBT in Table I, peak I, II, and III are mainly corresponding to the melt-crystallization behavior of PET, PBT, and PTT, respectively. Therefore, for B2 and B3 blends, each component of the PET, PTT, and PBT in the blend forms their own crystals during cooling scan.

For B4 blend, the exotherm exhibits two crystallization peaks: a major and sharper peak I at higher temperature and a subordinate peak III at lower temperature. The sharp peak I at high temperature may be attributed to the crystalline phase of mixed crystals of PBT and PET because of their closely melt-crystallization temperatures, and the subordinate peak I at lower temperature is attributed to the crystalline phase of PTT because of its much lower T_{ch}.

Furthermore, it is easy to find in Fig. 2(b) that peak I of the four blends (B2-B5) become shaper and the peak temperatures are increasing from 204.6 to 214.8°C with the increase of the PET content. While peak III of the four blends (B1-B4) become lower with increasing of the PET component.

On the other hand, it is easy to find that the peak area (corresponding to the crystallization enthalpy) and the shape of peak I decreases gradually and become less shaper with the decrease of the content of PET, and the peak area of peak III increases gradually with the increase of the content of PTT, which strongly confirmed that the assignments of the peaks is reasonable. Some researchers also reported the similar results about the binary or ternary blends during melt-crystallization process, the exotherm show a single peak when the minor component is less than a specific weight percentage, while it displays multiple peaks when the specific weight percentage of each component is close.[26–27]

Nonisothermal crystallization behaviors and kinetics

Nonisothermal crystallization behaviors

Figure 3(a,b) show the nonisothermal crystallization behaviors of B1 and B5 samples at various cooling rates, and the parameters are listed in Table III. From both melt-crystallization curves of B1 and B5

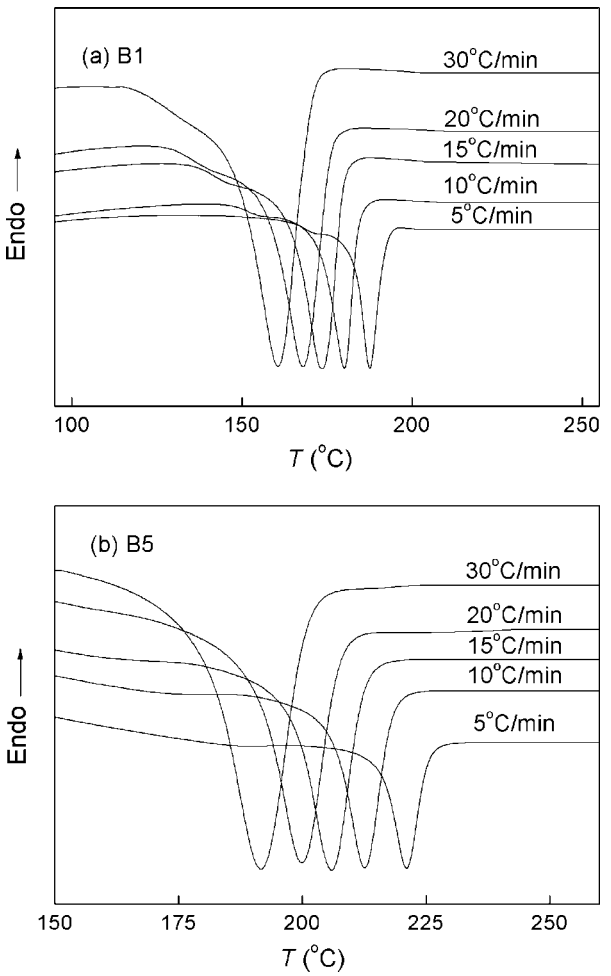

Figure 3 DSC crystallization curves of (a) B1 and (b) B5 blends at various cooling rates.

blends, it can be easily found that the DSC curves display only one exotherm peak, and this phenomenon also can be found in Figure 2(b), and no separate peaks are observed at each cooling rate, which is the reason why they are selected to study the nonisothermal crystallization. The mixed crystals may be dominantly containing PTT and PBT component for B1 blend, and containing PET and PBT component for B5 blend, respectively.

Generally speaking, the higher cooling rate, the later the crystallization starts, and the wider crystallization curves. As it is expected that the exothermic peaks' temperature decrease from 187.6 to 160.5°C for B1, from 221.1 to 191.7°C for B5, which is attributed to the low time scale that allows the polymer to crystallize with increasing cooling rate, thus requiring a higher supercooling to initiate crystallization, and the exotherms became broader with the increasing of the cooling rate from 5 to 30°C/min. When the specimens are cooled fast, the motion of the molecular chain in blends is not able to follow the cooling temperature, and then the molecular chains become less mobile and have short time to diffuse into the crystallite lattice and to adjust and organize the chain conformation into less perfect crystallites. As a result, the crystallization enthalpies (ΔH) of samples gradually decrease with the increasing of cooling rate for both B1 and B5 blends (Table III). Furthermore, the half-time of the crystallization ($t_{1/2}$) is gradually decreasing with increasing cooling rate for both blends, indicating a higher cooling rate, a faster crystallization rate; and the $t_{1/2}$ values of the B1 blend is larger than that of the B5 blend, which indicates that a faster crystallization rate for the sample with more PET content.

From DSC crystallization curves of the B1 and B5 blends, the relative crystallinity as a function of temperature for ternary blends at different cooling rates is shown in Figure 4(a,b). It can be seen that all these curves have similar sigmoidal shape, with a fast primary crystallization during the early stage and a slow secondary crystallization at the later stage. The curvature of the upper part plot is observed to level off because of the crystal impingement or crowding in the final stage of crystallization. In nonisothermal crystallization, the temperature scale can be transformed into the time scale by using Eq. (4). The plots of X_t versus t are shown in Figure 5(a,b). In this case, it is obvious that the values of $t_{1/2}$ are decreasing with the increase of cooling rate, suggesting that the sample crystallizes faster when the cooling rate is increased. By careful observation, the values of the $t_{1/2}$ are increased with increasing the PTT content at a given cooling rate, and the result indicates a decrease of the whole crystallization rate of the ternary blends with increasing PTT content.

TABLE III
Nonisothermal Crystallization Kinetic Parameters of B1 and B5 Blends Analyzed by Modified Avrami Equation

D	B1						B5					
(°C/min)	T_p (°C)	n	Z_t (10^{-8} s^{-n})	Z_c (s^{-n})	$t_{1/2}$ (s)	ΔH (J/g)	T_p (°C)	N	Z_t (10^{-8} s^{-n})	Z_c (s^{-n})	$t_{1/2}$ (s)	ΔH (J/g)
5	187.6	3.8	1.70	0.028	109.7	−41.3	221.1	3.5	4.57	0.034	110.3	−35.0
10	180.2	3.7	4.90	0.186	73.1	−38.1	212.6	3.6	5.01	0.186	72.9	−32.5
15	173.6	3.9	9.33	0.339	55.6	−36.4	206.0	3.6	24.55	0.363	55.4	−31.9
20	168.1	4.0	16.59	0.457	47.8	−35.7	199.9	3.4	114.81	0.501	44.6	−31.3
30	160.5	4.0	28.84	0.603	39.9	−35.3	191.7	3.7	117.49	0.631	36.4	−29.7

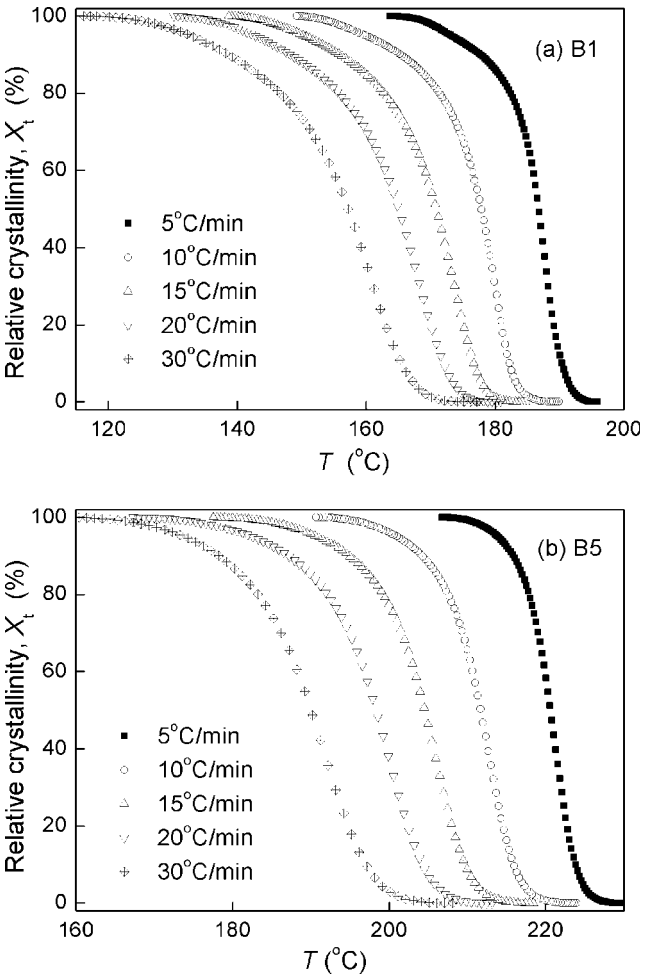

Figure 4 Relative crystallinity versus temperature for nonisothermal crystallization of (a) B1 and (b) B5 samples at various cooling rates.

Nonisothermal crystallization kinetics

Modified Avrami analysis. Assuming that the relative crystallinity (X_t) increases with the crystallization time (t), the modified Avrami equation can be used to analyze the nonisothermal crystallization process of the B1 and B5 ternary blends. Figure 6 is a double logarithm plot of Eq. (3)'s amorphous fraction and crystallization time at different cooling rates. Nonisothermal crystallization kinetic parameters analyzed by modified Avrami equation are shown in Table III. The Avrami exponent n and Z_t are obtained from the slopes and the intercepts, respectively. The plots of Figure 6 show good linearity except a secondary crystallization at the later crystallization stage. In this article, the attention is focused on the primary crystallization. The Avrami exponent n of ternary blends are found to range from 3.7 to 4.0 for B1 and from 3.4 to 3.7 for B5 when cooling rates increased from 5 to 30°C/min. The Avrami exponent, $n = 3.7 \pm 0.3$, suggest a thermal nucleation and a three-dimensional spherical growth mechanism.[28] It is known that the nucleation mode is dependent upon the cooling rate.[29] With the increase of the cooling rate, the value of n decreases gradually, implying that the nucleation mechanism changed from a thermal to an athermal mode. By carefully observation, it is easily to found that the n values of the B1 blend is larger than that of the B5 blend at a given cooling rate. The reason for this is that the crystallization rate of B1 blend is slower than that of the B5 blend, and more perfect crystallites in the B1 blend can be formed than B5. From Table III, the Avrami crystallization kinetic parameters, Z_t and Z_c, are found to increase with increasing cooling rate, suggesting a faster crystallization rate at higher cooling rate. Moreover, Z_t and Z_c of the B5 ternary blend at a given cooling rate is larger than that of the B1 blend, indicating a higher crystallization rate with more PET content in ternary blends.

Ozawa analysis. Since the nonisothermal crystallization is a rate-dependent process, Ozawa took into account the effect of cooling (or heating) rate, D, on

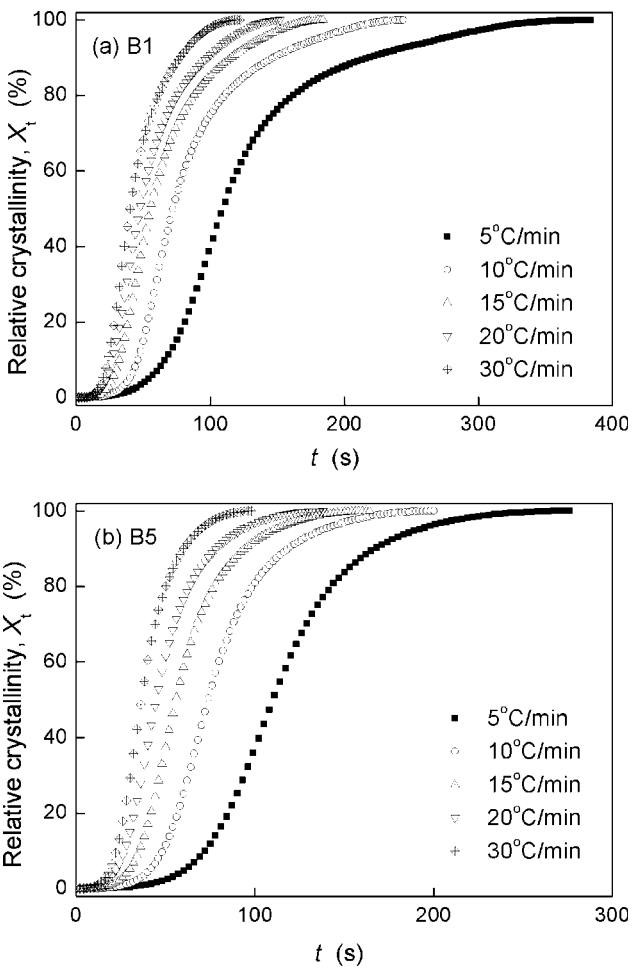

Figure 5 Relative crystallinity versus time for nonisothermal crystallization of (a) B1 and (b) B5 samples at various cooling rates.

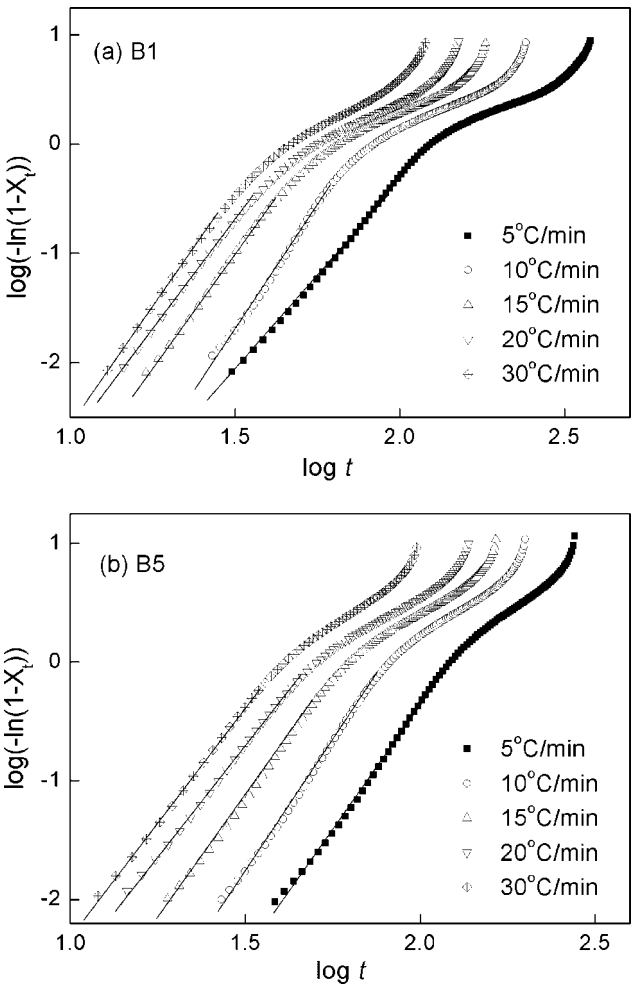

Figure 6 Plots of $\log[-\ln(1 - X_t)]$ versus $\log t$ for nonisothermal crystallization of (a) B1 and (b) B5 blends.

the crystallization process from the melt or glassy state, and modified the Avrami equation.

According to Ozawa's theory and plots of $\log[-\ln(1 - X_t)]$ versus $\log|D|$ at a given temperature, we will obtain a series of straight lines if Ozawa analysis is valid, and the crystallization kinetic parameters m and $\log K(T)$ can be derived from the slope and the intercept. The results of Ozawa analysis for both B1 and B5 ternary blends are shown in Figure 7(a,b). All lines are not straight with the change of cooling rate especially at higher cooling rate. On the other hand, the curvature of the lines show different tendency at different temperature, in which the higher the temperature is, the more is the curvature. Therefore, the accurate analysis of nonisothermal crystallization data could not be performed by Ozawa equation because of the variation in the slope with temperature. It means that the parameters m is not a constant during the nonisothermal crystallization process, and the Ozawa's approach is not suitable to describe the nonisothermal crystallization process although it has been provided a satisfactory description to the nonisothermal melt-crystallization for PTT/PBT blends.[15] Sajkiewicz et al.[30] report that the line function as predicted by Ozawa is observed only for data obtained at relatively low cooling rates. The nonisothermal crystallization of the PET/PTT/PBT ternary blends did not follow the Ozawa equation, probably because of the disregarded assumptions in Ozawa's theory.[31]

Crystal morphology

Crystal morphology of the blend B1-B5 is observed by POM and six images are obtained as shown in Figure 8(B1–B5), respectively. Within the volume between two glass plates with a distance about 200 μm, many distortional small Maltese crosses with the size of 10–30 μm can be observed in Figure 8(B1-B2), suggesting that the crystal morphology of B1 and B2 is a relative bad-defined spherulitic texture with distortional or hazy Maltese crosses. However, for B3-B5 samples, it is clear that many light spots

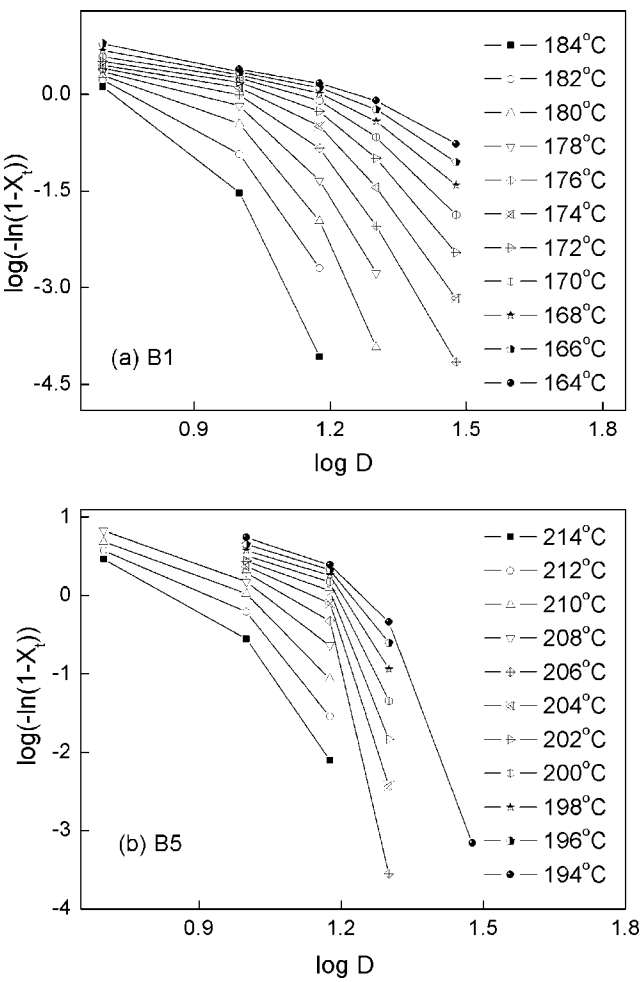

Figure 7 Ozawa plots of $\log[-\ln(1-X_t)]$ versus $\log D$ for nonisothermal crystallization of (a) B1 and (b) B5 ternary blends.

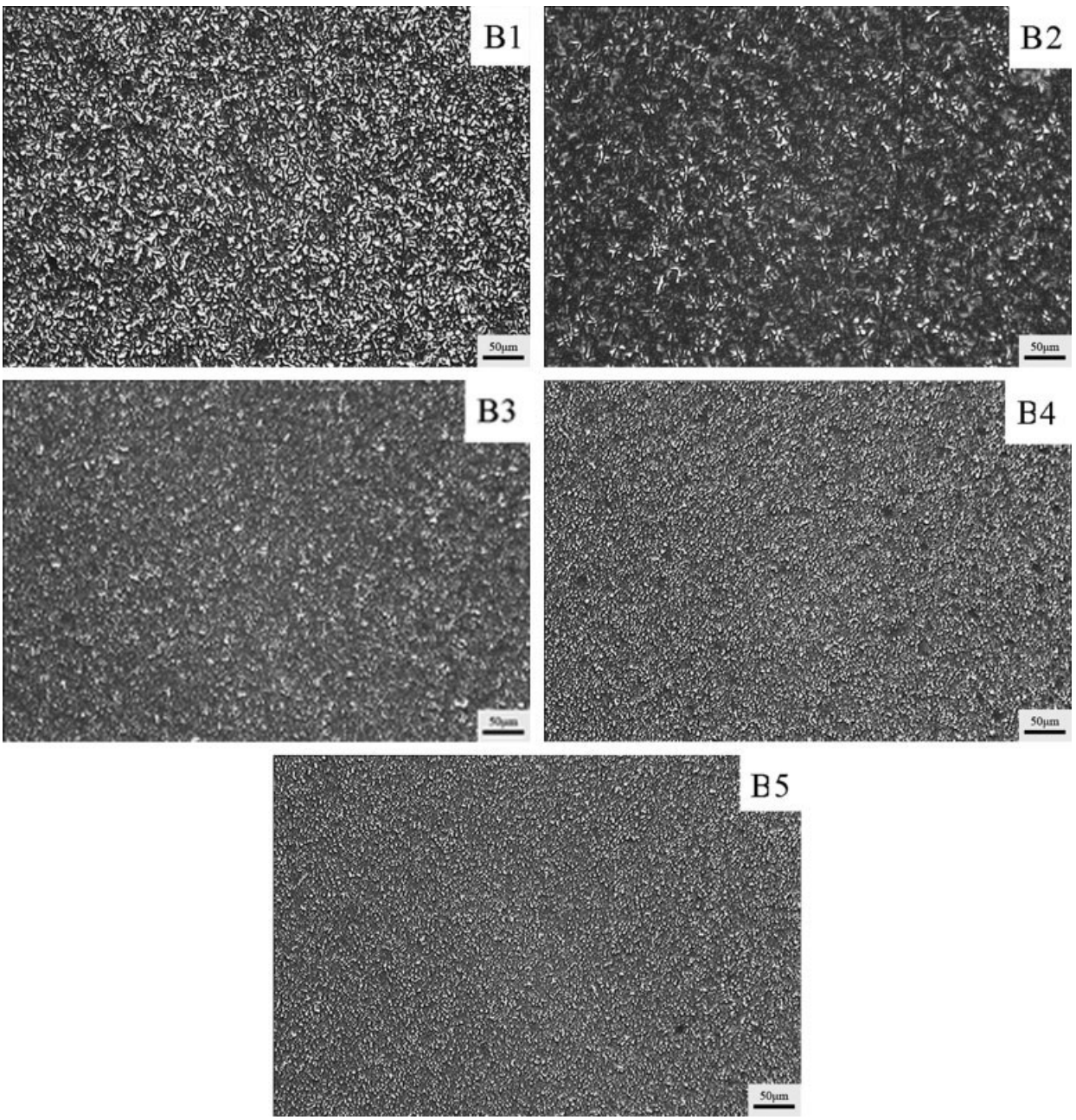

Figure 8 Polarized optical micrographs of PET/PTT/PBT blend.

become smaller and smaller with the increase of the PET component, indicating the dimension and the degree of perfection of crystallites are smaller and less perfect than those of B1 or B2. These results indicate that all of the ternary blends of PTT, PET, and PBT have a fast crystallization rate; therefore, no perfect crystal morphology can be formed during the melt-crystallization process. On the other hand, the blend, e.g., B1 and B2 with the major component of PTT that has a relative lower crystallization rate than PET in blend, has improved crystal morphology than those with the major component of PET in blend.

CONCLUSIONS

PET/PTT/PBT ternary blends prepared by melt-compound are investigated using DSC and POM. Different ternary blends show different melting and crystallization behaviors with varied content of PET/PTT in blends when the weight ratio of PBT is a constant. The PBT component improves the melt-crystallization temperature of the ternary blends. PET, PTT, and PBT components are miscible in amorphous state evidently for a single and composition-dependent glass transition temperature shown in the DSC thermograms. There are two melting

peaks for each ternary blend, in which peak I at higher temperature is corresponding to the melt of the crystals of PET, and peak II at lower temperature is corresponding to the melt of PBT and PTT or mixed crystals of PTT/PBT. Only one exotherm peak is shown in DSC curve when the weight ratio of PET/PTT/PBT are 10/50/30 (B1) and 50/10/30 (B5) because they crystallize simultaneously and form mixed crystals in the ternary blends. Three exothermic peaks are observed in the melt-crystallization curves when the ratios of PET/PTT/PBT are 20/40/30 (B2) and 30/30/30 (B3), which corresponds to the separated crystal phase of the PBT, PET, and PTT, respectively. Two exothermic peaks appear in the DSC curves when the weight ratio of the PET/PTT/PBT is 40/20/30 (B4), the peak at higher temperature is corresponding to mixed crystals of PBT and PET; and the peak at lower temperature is corresponding to the crystallization of PTT. The Avrami analysis of the ternary blend indicates that the nonisothermal process is composed of the primary stage and the secondary stage for both B1 and B5 blends. At the primary stage, the Avrami exponent n ranges from 3.7 to 4.0 for B1 and from 3.4 to 3.7 for B5 at various cooling rates, respectively. The crystallization rate parameters $t_{1/2}$ and Z_c suggest a lower crystallization rate of B1 with more PTT content in blends. The Ozawa equation is not suitable to describe the whole nonisothermal crystallization process because the parameters m is not a constant during the nonisothermal crystallization process. The crystal morphology of the five ternary blends show different size and distortional Maltese crosses or light spots when the PTT or PET component varies, and the blend with the more PTT content, the larger crystallites forms in ternary blends.

References

1. Whinfield, J. R.; Dickson, J. T. Brit. Pat. 578,079, (1946).
2. Wu, J.; Schultz, J. M.; Samon, J. M.; Pangelinan, A. B.; Chuah, H. H. Polymer 2001, 42, 7141.
3. Grande, J. A. Mod Plast 1997, 12, 97.
4. Apiwanthanakorn, N.; Supaphol, P.; Nithitanakul, M. Polym Test 2004, 23, 817.
5. Dangseeyun, N.; Supaphol, P.; Nithitanakul, M. Polym Test 2004, 23, 187.
6. Jafari, S. H.; Yavari, A.; Asadinezhad, A.; Khonakdar, H. A.; Böhme, F. Polymer 2005, 46, 5082.
7. Chuah, H. H. Polym Eng Sci 2001, 41, 308.
8. Hong, P. D.; Chung, W. T.; Hst, C. F. Polymer 2002, 43, 3335.
9. Xue, M. L.; Sheng, J.; Yu, Y. L.; Chuah, H. H. Eur Polym J 2004, 40, 811.
10. Kang, T. K.; Kim, Y.; Ha, C. S. J Appl Polym Sci 1999, 74, 1797.
11. Jacques, B.; Devaux, J.; Legras, R.; Nield, E. Polymer 1997, 38, 5367.
12. Song, K. J.; White, J. L. Polym Sci Eng 2000, 40, 902.
13. Yang, Y.; Li, S.; Brown, H.; Casey, P. AATCC 2002, 2, 54.
14. Ou, C. F.; Li, W. C.; Chen, Y. H. J Appl Polym Sci 2002, 86, 1599.
15. Supaphol, P.; Dangseeyun, N.; Srimoaon, P. Polym Test 2004, 23, 175.
16. Avarami, M. J Chem Phys 1940, 8, 212.
17. Jeziorny, A. Polymer 1978, 19, 1142.
18. Ozawa, T. Polymer 1971, 12, 150.
19. Dangseeyun, N.; Srimoaon, P.; Supaphol, P.; Nithitanakul, M. Thermochim Acta 2004, 409, 63.
20. Supaphol, P, Dangseeyun, N.; Srimoaon, P.; Nithitanakul, M. Thermochim Acta 2003, 406, 207.
21. Huang, J. M.; Chang, F. C. J Polym Sci Part B: Polym Phys 2000, 38, 934.
22. Chung, W. T.; Yeh, W. J.; Hong, P. D. J Appl Polym Sci 2002, 83, 2426.
23. Wu, P. L.; Woo, E. M. J Polym Sci Part B: Polym Phys 2003, 41, 80.
24. Dandurand, S. P.; Perez, S.; Revol, J. F.; Brisse, F. Polymer 1979, 20, 419.
25. Wang, B. J.; Christopher, Y.; Hanzlicek, J.; Cheng, S.; Geil, P. H.; Grebowicz, J.; Ho, R. M. Polymer 2001, 46, 7171.
26. Qiu, Z.; Ikehara, T.; Nishi, T. Polymer 2003, 44, 2503.
27. Qiu, Z.; Ikehara, T.; Nishi, T. Polymer 2003, 44, 3101.
28. Wunderlich, B. Macromolecular Physics; Academic Press: New York, 1976.
29. Choe, C. R.; Lee, K. H. Polym Eng Sci 1989, 29, 801.
30. Sajkiewicz, P.; Carpaneto, L.; Wasiak, A. Polymer 2001, 42, 5365.
31. Di Lorenzo, M. L.; Silvestre, C. Prog Polym Sci 1999, 24, 917.